

An Active Perception Game for Robust Information Gathering

Siming He, Yuezhan Tao, Igor Spasojevic, Vijay Kumar and Pratik Chaudhari

Abstract—Active perception approaches select future viewpoints by using some estimate of the information gain. An inaccurate estimate can be detrimental in critical situations, e.g., locating a person in distress. However the true information gained can only be calculated *post hoc*, i.e., after the observation is realized. We present an approach for estimating the discrepancy between the information gain (which is the average over putative future observations) and the true information gain. The key idea is to analyze the mathematical relationship between active perception and the estimation error of the information gain in a game-theoretic setting. Using this, we develop an online estimation approach that achieves sub-linear regret (in the number of time-steps) for the estimation of the true information gain and reduces the sub-optimality of active perception systems. We demonstrate our approach¹ for active perception using a comprehensive set of experiments on: (a) different types of environments, including a quadrotor in a photorealistic simulation, real-world robotic data, and real-world experiments with ground robots exploring indoor and outdoor scenes; (b) different types of robotic perception data; and (c) different map representations. On average, our approach reduces information gain estimation errors by 42%, increases the information gain by 7%, PSNR by 5%, and semantic accuracy (measured as the number of objects that are localized correctly) by 6%. In real-world experiments with a Jackal ground robot, our approach demonstrated complex trajectories to explore occluded regions.

I. INTRODUCTION

As robots transition from controlled laboratory environments to real-world settings, their ability to actively perceive information from their surroundings becomes increasingly crucial. Active perception has gained research interest due to its potential applications in search and rescue, planetary exploration, environmental monitoring, and structural inspection [1], [2].

Active perception is the task of identifying and navigating to viewpoints that maximize information gain. The notion of information gain can vary depending on the application. For example, in search and rescue, the robot may need to acquire the geometric information about a collapsing structure or collect photometric and semantic information to identify people in distress and assess their health conditions. Regardless of the specific definition, the “true” information gain is the incremental knowledge obtained from future observations. Since future observations are unknown *a priori*, the robot must rely on estimates to guide its decisions. Inaccurate estimates can lead the robot to select sub-optimal viewpoints. This issue is particularly critical in safety-sensitive applications such as search and rescue, where missing information—such as a person in distress—can have severe consequences.

This paper proposes an online procedure for estimating the actual information gain. The key mathematical idea is as

The authors are with the General Robotics, Automation, Sensing and Perception (GRASP) Laboratory, University of Pennsylvania. Email: {siminghe, yztao, igorspas, kumar, pratikac}@seas.upenn.edu.

¹Code is available at <https://github.com/grasp-lyrl/active-perception-game>.

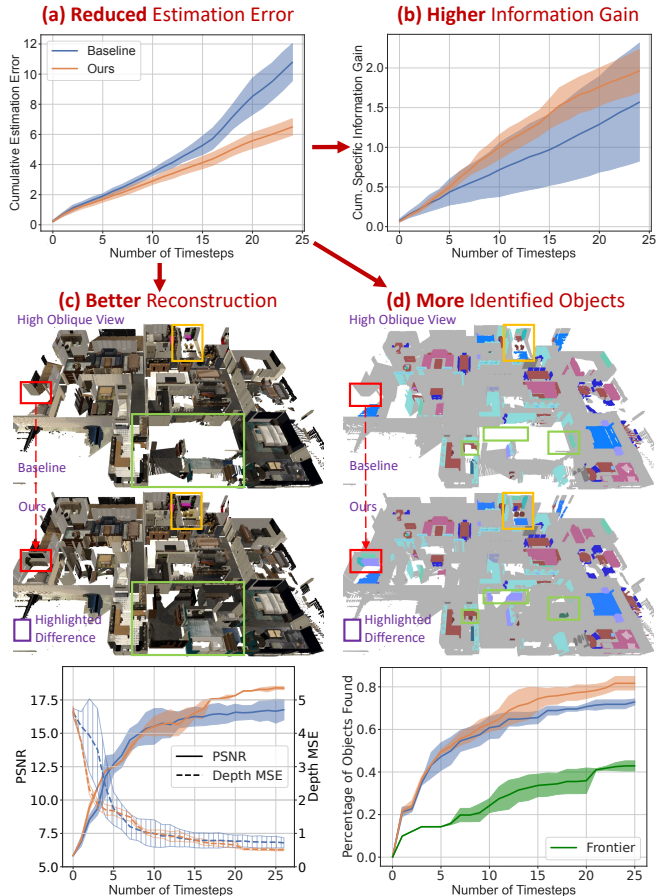


Fig. 1: Comparison of our approach for active perception against a baseline for a quadrotor exploring an indoor environment in a photorealistic simulator. Our approach reduces estimation errors (a), leads to a higher information gain (b), better reconstruction with higher peak signal-to-noise-ratio (PSNR) and lower depth mean square error (MSE) in the learned neural radiance field (NeRF) (c), and leads to an increase the total number of objects that are correctly localized in the scene (d).

follows. We model active perception as a game where the robot selects informative viewpoints while the adversarial player provides inaccurate estimates of the information gain at these viewpoints to mislead the robot. Since the environment is fixed, the adversarial player cannot cause arbitrarily large harm. We design an online optimization algorithm that allows the robot to learn from the discrepancy between its pre-observation estimates and the actual information gained after receiving the observations. This learning process enables the robot to fix its inaccurate estimates in the subsequent time-steps. This mathematical approach provides explicit guarantee on the regret of both (a) the quality of the estimated information gain $O(T^{3/4})$ in the length of the episode T , and (b) the quality of the entire active perception pipeline including informative path planning $O(T^{3/4} + \lambda T + \Delta)$ where λ and Δ will be described in detail later.

Our approach is very general. It can be used to improve the performance of any active perception procedure. We demonstrate our approach for active perception using a comprehensive set of experiments on: (a) different types of environments, including a quadrotor in a photorealistic simulation, real-world robotic data, and real-world experiments using ground robots exploring indoor and outdoor scenes; (b) different types of robotic perception data; and (c) different map representations.

II. RELATED WORK

Methods with performance guarantees: Active sensing in GP has been well studied in [3]. Finding optimal sensor placement has intractable runtime. The work obtains near-optimal online bounds for greedy algorithms based on the submodularity of mutual information. The analysis assumes GP has a known covariance function which is usually unrealistic in real-world applications. An extension [4] uses a near-optimal exploration-exploitation approach for stationary GP with an unknown covariance function. For non-stationary GP, a single estimation of covariance function is not enough. The paper [4] proposed manually dividing the whole space into smaller areas with a stationary process. Then, a similar analysis also gives an efficient and near-optimal algorithm for informative path planning in GP [5], [6], [7].

Methods without performance guarantees: Occupancy map is commonly used in robotics tasks, but active perception algorithms based on occupancy maps usually don't provide performance guarantee analysis. Next-best-views (NBV) methods samples and selects viewpoint that maximizes some utility functions. Utilities based on the amount of observed volume is used in [8], [9], [10]. The following works [11], [12] used surface reconstruction utility in addition to volumetric utility. Information-theoretic methods [13], [14], [15] design efficient algorithms to calculate mutual information between range sensor data and occupancy maps. Since the occupancy of unseen areas is unknown, NBV and information-theoretic methods could underestimate or overestimate the utility. To address this issue, several works [16], [17], [18] propose map completion. The methods train neural networks to predict the occupancy of unseen areas based on existing datasets. Semantic scene representations become popular in recent years and have been used for loop-closure, navigation, and decision making. Uncertainty in semantics [19], [20], [21] is used as a utility for exploration. Reinforcement learning methods [18], [22], [23], [24] are also used for active perception by learning to act based on past data.

Unlike GP in which the covariance function and information gain estimation are accurate, information gain estimations in occupancy map and semantic map are subject to uncertainties described in Section III-B. As a result, the information gain estimation could be inaccurate, and the performance guarantee would not hold. This gap motivates our design of accurate information gain estimator and analysis of performance guarantee for general scene representations.

III. METHOD

A. Problem Formulation

Let Θ denote a fixed scene from which a robot obtains a sequence of measurements $Y_1^t = (Y_1, \dots, Y_{t-1})$ from viewpoints $X_1^t = (X_1, \dots, X_{t-1})$ respectively where each $X_k \in \text{SE}(3)$

and each measurement Y_k is an RGBD image. We can write $p(Y_t | X_t, \Theta)$ as the probability of obtaining an observation Y_t from viewpoint X_t . At time t , the robot selects the next Δt viewpoints $X_t^{t+\Delta t}$ to obtain measurements $Y_t^{t+\Delta t}$. Access to measurements gives us information about the scene via the conditional probability $p(\Theta | Y_1^t)$.² The discrepancy between the intrinsic uncertainty of the scene $p(\Theta)$ and this conditional probability (averaged over past measurements) is given by the mutual information

$$I(\Theta; Y_1^t) = \int dp(y_1^t) \text{KL}(p(\Theta | y_1^t), p(\Theta)) \quad (1)$$

where $\text{KL}(\cdot, \cdot)$ denotes the Kullback-Leibler divergence, and I denotes mutual information. The expected information gain, i.e., the incremental amount of information obtained from new measurements (given past ones y_1^t) is

$$r_t \triangleq I(\Theta; Y_t^{t+\Delta t} | y_1^t) = H(\Theta | y_1^t) - H(\Theta | Y_t^{t+\Delta t}, y_1^t). \quad (2)$$

where H denotes the Shannon entropy.³ It is important to emphasize that expected information gain is a function of the past measurements that were realized y_1^t , not the random variable Y_1^t . It is also a function of the distribution of the future viewpoints $X_t^{t+\Delta t}$ chosen by the robot. To emphasize:

$$r_t \equiv r_t(X_t^{t+\Delta t} | y_1^t).$$

At each time-step, the robot selects future viewpoints using past measurements $p(X_t^{t+\Delta t} | y_1^t)$ to maximize the information gain. It solves the optimization problem

$$\underset{p(X_t^{t+\Delta t} | y_1^t)}{\text{maximize}} \quad r_t \quad (3)$$

by estimating the information gain.

The key idea of this paper is as follows. After visiting future locations $x_t^{t+\Delta t}$, the robot obtains new measurements $y_t^{t+\Delta t}$. It can now calculate the specific information gain, i.e., the realized reduction of uncertainty about the scene,

$$r_t^* \triangleq H(\Theta | y_1^t) - H(\Theta | y_t^{t+\Delta t}, y_1^t); \quad (4)$$

note the difference with respect to (2) where the conditioning is on $Y_t^{t+\Delta t}$. The discrepancy

$$\Delta r_t = r_t - r_t^* = H(\Theta | Y_t^{t+\Delta t}, y_1^t) - H(\Theta | y_t^{t+\Delta t}, y_1^t). \quad (5)$$

will lead to a suboptimal choice of viewpoints. In addition to the expected information gain r_t , the robot can estimate—in hindsight—the discrepancy and thereby hope to maximize a quantity closer to the specific information gain in the next step.

B. Estimating the specific information gain

The robot's estimate of the specific information gain r_t^* given the expected information gain r is denoted by

$$\hat{r}^* = f(s, r), \text{ where } f: \mathbb{N} \times \mathbb{R} \mapsto \mathbb{R}. \quad (6)$$

This function f , which we call the **improvement function**, is fitted using past expected information gains r_1^t and past

²We will use capital letters X, Y to denote random variables and small letters x, y to denote their corresponding values.

³Note that $H(\Theta | y_1^t) = -\int dp(\theta | y_1^t) \log p(\theta | y_1^t)$ while $H(\Theta | Y_t^{t+\Delta t}, y_1^t)$ equals

$$-\int dp(y_t^{t+\Delta t} | y_1^t) dp(\theta | y_t^{t+\Delta t}, y_1^t) \log p(\theta | y_t^{t+\Delta t}, y_1^t).$$

discrepancies Δr_1^t . We need to estimate this discrepancy in an online fashion. This is the why the function f depends on time s . The discrepancy between expected information gain and specific information gain is caused by:

- (a) Correlations in successive observations: If the robot chooses the next Δt viewpoints independently, its estimate of $I(\Theta; Y_t^{t+\Delta t} | y_1^t)$ in (2) will be computed using $\sum_{i=0}^{\Delta t-1} I(\Theta; Y_{t+i} | y_1^t)$. The two are not identical when observations are correlated with each other, e.g., when views overlap. In general, the latter is an overestimation. We design a non-parametric estimator for the specific information gain in (6) that will break the correlations in observations.
- (b) Model (epistemic) uncertainty: Our representation of the scene Θ is learned from past observations. If the representation is not capable enough to accurately capture the true scene, the estimate of $H(\Theta | y_1^t)$ could be incorrect. Estimating the specific information gain helps address this model uncertainty.
- (c) Data (aleatoric) uncertainty: For a dynamic scene, say a propeller with spinning blades, each voxel is occupied or not occupied with a probability that depends upon the angular velocity of the blade. The expected information gain will always be high but the specific information gain is quite low, i.e., after receiving the future observation, the location of the blade is known, up to motion blur. A robot that maximizes the expected information gain will never look away from the scene even if there is not much information to gleaned from it. Estimating the specific information gain also helps address the data uncertainty.

Representing the improvement function: We query the improvement function $f(s, r)$ in (6) to estimate specific information gain of future viewpoints corresponding to a horizon of length Δt , so the first argument has domain $s \in \{0, \dots, \Delta t - 1\}$. Let us suppose that the expected information gain is upper bounded by β , and therefore the domain of the second argument is $[0, \beta] \subset \mathbb{R}$ which we discretize into b equal-sized bins $[(k-1)\beta/b, k\beta/b)$ for $k \in \{1, \dots, b\}$. We can now represent the function f as a matrix

$$f \in \mathbb{R}^{\Delta t \times b}. \quad (7)$$

This matrix is updated by the robot after every Δt observations using the specific information gain as follows. The robot maintains a variable

$$\alpha_{s,i} = \sum_{s'=1}^t \mathbb{1}\{r_{s'} \in \text{bin } i\} \quad \forall s \in [t, t + \Delta t - 1].$$

The improvement function is updated for all $s \in [t, t + \Delta t - 1]$ and all $i \in \{1, \dots, b\}$ as

$$f_{s,i} \leftarrow r_{s,i} + \sqrt{\frac{\alpha_{s-\Delta t,i}}{\alpha_{s,i}}} (f_{s,i} - r_{s,i}) - \frac{\beta \text{sign}(f_{s,i} - r_{s,i}^*)}{4\sqrt{\alpha_{s,i}}} \quad (8)$$

where $r_{s,i}$ highlights that the information gain at timestep s is in the bin i . The next section proves that this update rule for the improvement function achieves sublinear regret $O(T^{3/4})$ for estimating the specific information gain. The first term is the most elementary estimate of the specific information gain; it is simply $r_{s,i}$. The second term downweights the influence of prior learning, allowing the third term to emphasize the current update. The third term fixes the discrepancy between the estimated specific information gain and the actual specific information gain in hindsight, with a weight that is proportional

to the learning rate to the element $f_{s,i}$ of the matrix f .

Selecting viewpoints using the estimated specific information gain Viewpoints X_t should be selected using (3) where r_t is replaced by the estimation of specific information gain in (8). But, even if we have a more accurate estimate of the information gain now, the optimization problem in (3) (also called the ‘‘informative path planning problem’’) is computationally intractable. There is existing work that has studied such problems to obtain near-optimal algorithms [3]. For instance, the eSIP algorithm in [5] selects viewpoints X_t that satisfy

$$\sum_{t=1}^T r_t^*(X_t | y_1^t) \geq \frac{(1-1/e)}{(1+\log_2 \Delta t)} \sum_{t=1}^T r_t^*(X_t^* | y_1^t),$$

where X_t^* is the optimal solution of the optimization problem and e is Euler’s number 2.718. We will see in the next section that if our viewpoint selection also satisfies a similar inequality:

$$\sum_{t=1}^T r_t^*(X_t | y_1^t) \geq \gamma \sum_{t=1}^T r_t^*(X_t^* | y_1^t)$$

for some $\gamma \in (0, 1]$, then we can bound the sub-optimality of the information gain of our approach (which estimates the specific information gain r_t^* using the expected information gain r_t) to be $O(T^{3/4} + \lambda T + \Delta)$. Here λ is characterizes the average discrepancy between the specific and expected information gain across the scene. The additive term Δ is the regret coming from approximate informative path planning.

IV. ANALYSIS

We model the discrepancy Δr_t as an adversary, meaning that it can significantly mislead active perception algorithms if decisions rely solely on r_t . Treating the discrepancy as adversarial allows the analysis to hold under minimal assumptions. We frame active perception as a game between the robot and this adversary: the robot aims to navigate to the most informative viewpoints, while the discrepancy attempts to mislead it. Our algorithm’s analysis is grounded in this game-theoretic framework.

A. Bound on regret of online estimation with full feedback

We first analyze our algorithm in a full-information setting, where the specific information gain is received for all possible paths. We will then demonstrate a reduction from the actual setting where specific information gain is received only for the path executed by the robot, this is the so-called bandit feedback.

Each element of the matrix f is learned independently, so we focus the analysis on a single element $f_{s,i}$. We skip time-steps that do not update $f_{s,j}$ and denote the others using $a \in \{1, \dots, \alpha_{s,i}^*\}$ where $\alpha_{s,i}^*$ is the total number of updates to $f_{s,i}$. For brevity, we will use shorthand f_a (improved estimate), r_a (elementary estimate), r_a^* (specific gain), α_a (number of updates), and d_a (sign of the error $f_{s,i} - r_{s,i}^*$) (8). These quantities change with time.

Let $\delta_a \equiv f_a - r_a$. Online prediction in the full-information setting is modeled as an online convex optimization problem. For each timestep a , the robot selects δ_a to minimize the loss $\ell_a = |\Delta r_a - \delta_a|$. When the robot finishes active perception and looks back, it realizes δ^* is the estimation that it should have made. Regret is the additional loss incurred by estimating δ_a

instead of δ^* :

$$\rho_{s,i} = \sum_{a=1}^{\alpha_{s,i}^*} \ell_a - \ell^* \text{ where } \ell^* = \min_{\delta^*} \sum_{a=1}^{\alpha_{s,i}^*} |\Delta r_a - \delta^*| \quad (9)$$

The overall regret is

$$\rho = \sum_{s=1}^{\Delta t} \sum_{i=1}^b \rho_{s,i}. \quad (10)$$

The update rule in (8) is a special case of “follow the regularized leader”, see Lemma 7.1 in the Appendix. This can be used to bound the regret in Lemma 7.2 in the Appendix, which leads to the following theorem.

Theorem 4.1: For the “follow the regularized leader” learning rate $\eta_a = \beta/\sqrt{\alpha_a}$ in (8), the regret is

$$\rho_{s,i} \leq \beta(N\sqrt{\alpha_{s,i}^*} + 1) \leq \beta(N\sqrt{T} + 1),$$

where the robot selects from among N candidate viewpoints at each timestep. The bound on ρ is in worst case $\Delta t b \beta(N\sqrt{T} + 1)$. To prove, plug in the specified η_a to the bound in Lemma 7.2. The regret $\rho_{s,i}$ is bounded due to Holder’s inequality $\sum_{s=1}^{\Delta t} \sqrt{1/s} \leq 2\sqrt{\Delta t}$.

B. Bound on regret of online estimation with bandit feedback

Using the approach of [25], bandit-feedback setting can be reduced to the full-information setting. For $a = 1, \dots, \alpha_{s,i}^*$, let the probability that x_a is on the executed path be p_a . The hallucinated loss $\hat{\ell}_a$ is

$$\hat{\ell}_a = \frac{|\Delta r_a - \delta_a|}{p_a} \mathbb{1}(x_a \text{ is executed}) \quad (11)$$

This loss is an unbiased estimator of the actual loss, as $\mathbb{E}(\hat{\ell}_a) = p_a |\Delta r_a - \delta_a| / p_a + 0 = |\Delta r_a - \delta_a|$. Additionally, to ensure that this loss is well-defined, we require p_a to be strictly positive. We can achieve this by randomly sampling paths with probability $\tau \in (0, \frac{1}{2})$ in the active perception algorithm.⁴ Since a feasible y_a must be included in at least one possible path, y_a is selected with a probability of at least $N^{-\Delta t}$. Given that the algorithm randomly samples paths with probability τ , p_a is greater than or equal to $\tau N^{-\Delta t} \geq 0$. Intuitively, in the bandit-feedback setting, the robot explores the specific information gain of different measurements via randomization. After randomization, we prove the expected regret in bandit-feedback setting in Lemma 7.3 in the Appendix. With randomization, the algorithm has sub-linear estimation regret:

Theorem 4.2: For $\tau = T^{-1/4}$, the regret bound is

$$\mathbb{E}(\rho_{s,i}) \leq N^{\Delta t} \beta(N T^{3/4} + T^{1/4}) + \beta T^{3/4} = O(T^{3/4}). \quad (12)$$

The overall regret is also $O(T^{3/4})$.

To prove, plug in the specified τ into the bound in Lemma 7.3.

C. Regret of active perception

This section characterizes the relationship between errors in estimation of the specific information gain, optimality of path planning, and the performance of active perception. We define the additional information gain that could be obtained if the robot plans optimal paths based on specific information gain r_t^* as the active perception regret:

$$\varrho = \sum_{t=1}^T \left[r_t^* \left(\hat{X}_t^{t+\Delta t} \right) - r_t^* \left(X_t^{t+\Delta t} \right) \right] \quad (13)$$

⁴These randomly sampled paths are necessary for the randomization-based reduction. In practice, the robot does not implement these random paths.

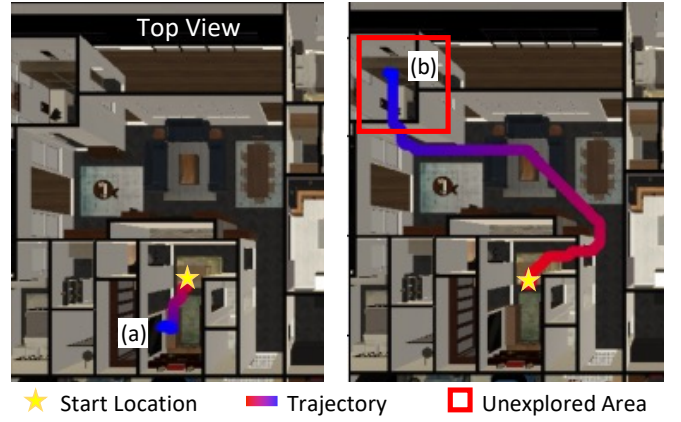


Fig. 2: Viewpoint selection comparison. Given a set of candidate trajectories, our method selects trajectory (b), which leads to an underexplored room, while the baseline selects trajectory (a), which remains within the same room.

where the viewpoints $\hat{X}_t^{t+\Delta t}$ are selected by maximizing specific information gain and $X_t^{t+\Delta t}$ are selected by maximizing the estimates of specific information gain. We first show that our estimations of specific information gain lead to bounded active perception regret.

Theorem 4.3: Given estimation regret bound ρ , the bound on active perception regret is given by

$$\mathbb{E}(\varrho) \leq 4(\rho + \rho') \quad (14)$$

where ρ' bounds the discrepancy between specific and expected information gain.

The bound ρ is shown in Theorem 4.2 to be sub-linear. If ℓ^* in (9) is bounded by λ , then we have $\rho' \leq nbT\lambda$.

Then, we can take the optimality of path planning algorithms into account.

Theorem 4.4: Given an IPP algorithm which selects $X_t^{t+\Delta t}$ with $\sum_{t=1}^T r_t^*(X_t | y_1^t) \geq \gamma \sum_{t=1}^T r_t^*(X_t^* | y_1^t)$, the active perception regret is

$$\mathbb{E}(\varrho) \leq 4(\rho + \rho') + \Delta \quad (15)$$

where $\Delta = (1 - \gamma) \sum_{t=1}^T r_t^*(\hat{X}_t^{t+\Delta t})$.

Remark 4.1: With optimal path planning, active perception regret bound is $O(T^{3/4} + \lambda T)$. And with approximate path planning, the regret bound is $O(T^{3/4} + \lambda T + \Delta)$.

V. EXPERIMENTAL VALIDATION

To evaluate the effectiveness and generalizability of our approach, we conducted experiments on two active perception systems: (i) a semantic neural radiance field (NeRF)-based active perception system on a quadrotor in a photorealistic simulator described in Section V-A, and (b) an occupancy map-based active perception system on a ground robot. We tested the effectiveness of our approach for online estimation of specific information gain using a real-world dataset (described in Section V-B). Finally, we demonstrate real-world experiments with the ground robot with all our algorithms running fully onboard in Section V-C.

A. Simulation experiments

1) *Setup:* Neural radiance fields (NeRFs) build a map of the environment capable of rendering images from new viewpoints [26]. We build upon the work of [20] which built a semantic NeRF that can also predict semantic segmentation maps. We do not go into the details of the architecture for lack of space, the reader is encouraged to read these two original

	Simulation Scene 2			Simulation Scene 3			Simulation Scene 4		
	Frontier	Baseline	Ours	Frontier	Baseline	Ours	Frontier	Baseline	Ours
Error ¹	-	3.90 ± 0.55	2.95 ± 0.28	-	7.85 ± 4.52	3.88 ± 1.63	-	3.22 ± 0.39	2.44 ± 0.18
Info. Gain ²	-	1.87 ± 0.18	1.90 ± 0.23	-	1.25 ± 0.15	1.29 ± 0.22	-	1.58 ± 0.15	1.54 ± 0.01
PSNR ↑	-	19.53 ± 0.65	20.73 ± 0.46	-	16.68 ± 0.89	17.12 ± 0.65	-	15.11 ± 0.22	15.29 ± 0.26
Depth MSE	-	0.62 ± 0.07	0.54 ± 0.07	-	0.89 ± 0.24	0.85 ± 0.25	-	1.09 ± 0.09	1.13 ± 0.09
# Objects (%) ³	62.60 ± 3.00	78.00 ± 7.20	86.20 ± 2.30	55.90 ± 12.0	77.50 ± 2.00	77.50 ± 1.10	62.00 ± 9.00	88.40 ± 3.80	89.90 ± 2.90

¹ The mean absolute error of specific information gain estimation. ² The mean of specific information gain. ³ The percentage of objects successfully located.

TABLE I: Quantitative performance comparison across additional simulation scenes. These results complement Fig. 1, further demonstrating the effectiveness of our method in terms of estimation error, information gain, reconstruction, and object identification, as detailed in Section V-A.

papers.⁵ Our goal in this experiment will be to demonstrate the improvements in the quality of the trained semantic neural radiance field (NeRF) using our approach for active perception.

We use a photorealistic 3D simulator called Habitat-Sim [27], [28], [29]. The robot starts at a random location in the map and collects an initial set of measurements to initialize the map. The exploration phase begins after this initialization. At each time-step, we sample 20 different locations on the 2D plane, generate paths to these locations using Dijkstra’s algorithm, and discretize each path into Δt steps to calculate the estimated specific information gain. The path with the highest information gain estimates is used to generate a dynamically feasible trajectories for the quadrotor using Rotorpy [30].

An ensemble of NeRFs is used to represent the scene Θ . We calculate the information gain independently for the different observation modalities (RGB, depth, semantic segmentation, and transmittance along a ray which is calculated from depth) and sum them up to estimate the total specific information gain. The number of bins b is set to 100, and the number of measurements Δt is set to 40. After execution the path to the chosen viewpoints, the robot computes specific information gain and updates the NeRF in an online fashion using the realized observations.

2) *Baselines and Metrics:* We conducted experiments with frontier based exploration [31], the approach of [20] which maximizes the expected information gain and our proposed approach (which estimates the specific information gain) on four simulated environments of varying sizes and complexities. The results are shown in Fig. 1 and Table I. Each experiment is repeated three times with the same initialization to obtain the mean and standard deviation of all performance measures. For each experiment, we recorded the mean absolute error of estimation of specific information gain, the mean of specific information gain, peak signal-to-noise ratio (PSNR) and depth mean square error (MSE) of NeRF, and the percentage of objects found during the experiment was recorded.⁶

3) *Results:* The proposed approach reduced the error of estimation by 24.2% - 50.6%, gathered 0% - 25.6% more information, and located 0% - 12% more objects compared to the baseline approaches. Compared to frontier-based exploration

⁵Observations $y_t^{t+\Delta t}$ include RGB images, depth measurements and semantic segmentations. We model the color and depth of each ray as a Gaussian distribution estimated from the ensemble. For calculating quantities like $H(\Theta | y_t^t)$, we use estimates of the entropy for these Gaussians. For instantiating our approach with its theoretical guarantees, these quantities should be bounded. We therefore clip the entropy (to a maximum value of 5). Semantic segmentation generates a distribution over categories and its entropy is already bounded. The transmittance of a ray is modeled as a Bernoulli random variable indicating whether the ray hits an obstacle, with entropy between 0 and 1.

⁶We do not use coverage because our approach maximizes photometric, geometric and semantic information recovered from the scene and not the area covered.

Noise Type →	Indoor: building_loop			Outdoor: penno_short_loop		
	None	Gaussian	Impulse	None	Gaussian	Impulse
Baseline	0.475	0.484	0.490	0.474	0.484	0.488
Ours	0.163	0.160	0.162	0.162	0.163	0.172

TABLE II: Estimation improvement for M3ED dataset. We compare the mean estimation errors of the baseline and our methods under different types of depth measurement noise described in Section V-B.

with a random frontier, our approach located 37.7% to 100% more objects. For NeRF reconstructions, our approach achieved 1.2% to 9.7% higher PSNR and -3.7% to 29.2% lower depth MSE across four scenes. Additionally, our approach has smaller standard deviations for most metrics, which demonstrates that it is consistently better. The advantage of our approach is clearer in Scene 1 and Scene 2 which are larger and more complex. We believe that approaches like ours for estimating the specific information gain are more effective for environments that are large in scale and complexity.

Qualitatively, Fig. 1(c) compares explored areas by different approaches. Several rooms that were missed by the baseline are explored by our approach. Fig. 1(d) compares the objects located by the baseline and by our approach. Objects of different categories are associated with different colors. Our approach identifies more objects, including small chairs under the table and a toilet in a small bathroom. In Fig. 2, we give an example of viewpoint selection by baseline and our approach. In one of the timestep, the robot samples a set of candidate trajectories and select the trajectory with highest information gain. By better estimating the specific information gain, our approach selects a trajectory to an underexplored room.

B. M3ED Dataset

M3ED [32] is a high-quality dataset that consists of a large set of natural scenes including cars driving in urban, forest, day and night conditions. Since this data is already collected, we cannot perform “exploration” in it. But we can use it to evaluate our approach for estimating the specific information gain. This is important because it shows that we can demonstrate our approach on real-world data.

1) *Setup:* We use a 3D occupancy-map-based map in this section (instead of a NeRF like the previous section). We treat LiDAR data as the ground-truth depth, and LiDAR-based odometry in M3ED as the ground-truth location of the robot. All voxels are initially assigned a probability of occupancy of 0.5. For each measurement and its associated odometry, ray-casting was performed, followed by a log-odds-based map update. To calculate the information gain, rays were uniformly sampled from each viewpoint. Given depth measurements y_t and the sensor model, we calculated the information gain as $H(\Theta) - H(\Theta | y_t)$, where $p(\Theta)$ and $p(\Theta | y_t)$ represent the probability of occupancy before, and after, map update. Information gain is the sum of information gains from all sampled rays at the given viewpoint. After each

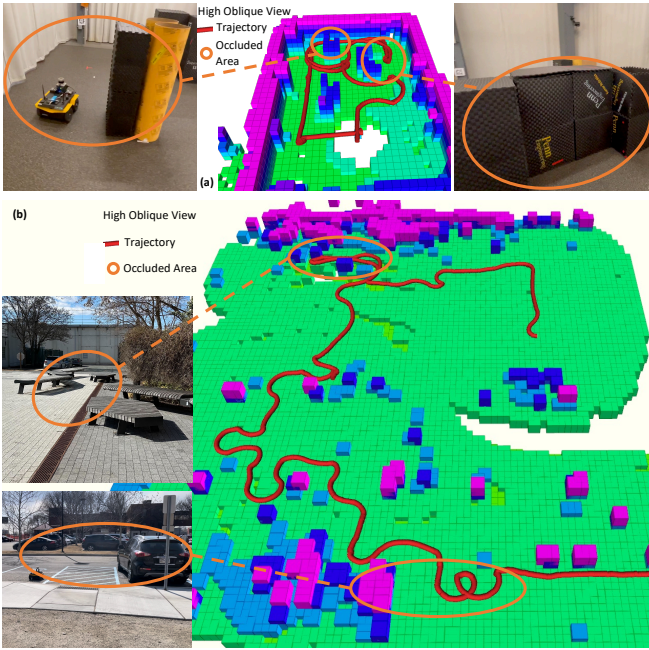


Fig. 3: Reconstructed Occupancy Map and Exploration of Occluded Areas in Real-World Experiment. The robot navigates to occluded areas, highlighted by orange circles, in indoor (a) and outdoor (b) environments.

realized observation, we calculated the specific information gain and the mean estimation error in the map occupancy. For this experiment, the upper bound on entropy $\beta = 1$, the number of bins $b = 100$, and $\Delta t = 1$.

2) *Results:* Our approach reduces the error of estimating the specific information gain estimations by over 66% in both indoor and outdoor scenes in M3ED dataset. See Table II.⁷

C. Real-world experiments on ground robots

1) *Setup:* We use a customized Clearpath Jackal platform, details can be found in [33], equipped with an AMD Ryzen 3600 CPU, an Nvidia GTX 1650 GPU and an Ouster OS1-64 LiDAR. We used Faster-LIO [34] for state estimation and move-base [35] for global and local planning. All real-world experiments use the same map representations and definition of information gain as those in Section V-B, except that we use a horizon of $\Delta t = 5$ to reduce the computational load and enable real-time operation. At each timestep, we sampled a 11×11 grid centered around the robot, with a cell size of 2×2 meters, to calculate the information gain at each cell lattice. The path with the maximum specific information gain estimate was obtained using depth first search on the grid, with a maximum length of 10 meters.

2) *Results:* We carried out experiments in both an indoor environment and an urban outdoor environment. One representative result in each environment is shown in Fig. 3. In the indoor environment in Fig. 3(a), the robot actively navigated to the occluded regions behind the barriers. In outdoor environment in Fig. 3(b), the robot actively navigated to occluded areas, e.g., the region between benches and the

⁷Unmodeled noise can introduce aleatoric uncertainty, which is often underestimated in information gain predictions. We added Gaussian noise (zero mean, standard deviation equal to $1/8^{\text{th}}$ of the raw depth) and Impulse noise (half of the LiDAR observations are replaced with random values between $1/3$ and $5/3$ of the raw depth) to simulate unmodeled sensor noise in LiDAR data. Table II shows that the proposed approach significantly improves the estimate of the information gain for unmodeled sensor noise.

parking lot occluded by the cars. Areas with high information gain are highlighted. With the proposed approach running online, the robot was able to actively plan paths to maximize the gathered information, resulting in full coverage of areas with high information content.

VI. CONCLUSION

Active perception is difficult because the robot has to estimate the actual information that will be gleaned, this gain can only be measured *post hoc*, after observations are realized. This paper demonstrates an online approach to estimate this *post hoc* information gain using the expected information gain. This estimator is critical for instantiating any active perception system. We obtained a mathematical characterization of the improvement in active perception using such an estimator. We demonstrated our approach for online information gain estimation on a comprehensive set of simulation and real-world experiments. Our approach is capable of building better photometric, geometric and semantic maps using different kinds of robotic perception data in indoor and outdoor environments.

VII. ACKNOWLEDGMENTS

We gratefully acknowledge the support of NIFA grant 2022-67021-36856, NSF grants 2112665, 2415249, IIS-2145164, CCR-2112665, and the IoT4Ag ERC funded by the National Science Foundation grant EEC-1941529. Siming He acknowledges the support of the Wharton Summer Program for Undergraduate Research.

APPENDIX

Lemma 7.1: Follow the regularized leader with a regularization of δ_a^2/η_a results in the update rule:

$$\delta_a = \frac{\eta_a}{\eta_{a-1}} \delta_{a-1} + \frac{\eta_a}{2} d_a, \quad (16)$$

where η_a and η_{a-1} are the learning rates for the current and previous updates, respectively.

In “follow the regularized leader”, $\delta_a = \arg \min_{\delta} \sum_{i=1}^t [\delta(-d_a) + \delta^2/\eta_a]$. We obtain (16) after finding minimizers δ_a and δ_{a-1} .

Lemma 7.2: Follow the regularized leader with regularization δ_a^2/η_a has the following regret bound.

$$\rho_{s,i} \leq \sum_{i=1}^{\alpha_{s,i}^*} \frac{N\eta_a}{2} + \frac{\beta^2}{\eta_1} \quad (17)$$

We know that $\rho_{s,i} \leq \sum_{i=1}^{\alpha_{s,i}^*} (\delta_a - \delta^*) d_a$ by convexity. We decompose the bound into two parts: 1) $\sum_{i=1}^{\alpha_{s,i}^*} \delta_{a+1} d_a - \delta^* d_a \leq \beta^2/\eta_1$ by Lemma 1.4.1 and Lemma 1.4.2 in [36]; 2) $\sum_{i=1}^{\alpha_{s,i}^*} \delta_a d_a - \delta_{a+1} d_a \leq \sum_{i=1}^{\alpha_{s,i}^*} |\delta_a - \delta_{a+1}| |d_a| \leq \sum_{i=1}^{\alpha_{s,i}^*} N\eta_a/2$.

Lemma 7.3: $\mathbb{E}(\rho_{j,k}) \leq N\beta(N\sqrt{T} + 1)/\tau + \tau\beta T$.

With probability $(1 - \tau)$, the full-information algorithm with filled loss gives bound $N^{\Delta t} \beta/\tau(N\sqrt{T} + 1)$ by Theorem 4.1. With probability τ , the regret bound is βT . Then, we get the expected regret.

Proof Sketch of Theorem 4.3: Let \bar{r}_a be $r_{a,s} + \arg \min_{\delta} \sum_{a=1}^s |\Delta r_a - \delta|$ and \bar{X}_a be $\arg \max_X \bar{r}_a(X)$. Let \hat{r}_a be $r_a + \delta_a$. We decompose $r_a^*(X_a^*) - r_a^*(X_a)$ into $[r_a^*(X_a^*) - \bar{r}_a(X_a^*)] + [\bar{r}_a(X_a^*) - \bar{r}_a(\bar{X}_a)] + [\bar{r}_a(\bar{X}_a) - r_a^*(\bar{X}_a)] + [r_a^*(\bar{X}_a) - \bar{r}_a(\bar{X}_a)] + [\bar{r}_a(\bar{X}_a) - \hat{r}_a(\bar{X}_a)] + [\hat{r}_a(\bar{X}_a) - \hat{r}_a(X_a)] + [\hat{r}_a(X_a) - \bar{r}_a(X_a)] + [\bar{r}_a(X_a) - r_a^*(X_a)]$. We have $\mathbb{E}[\sum_{t=1}^T \hat{r}_t(X_t) - \bar{r}_t(X_t)] = \mathbb{E}[\sum_{s=1}^{\Delta t} \sum_{i=1}^b \rho_{s,i}] \leq \rho$ and

$\sum_{s=0}^{\Delta t-1} (\hat{r}_{t+s}(\bar{X}_{t+s}) - \hat{r}_{t+s}(X_{t+s})) = \sum_{s=0}^{\Delta t-1} [\hat{r}_{t+i}(\bar{X}_{t+s}) - \max_X \hat{r}_{t+s}(X)] \leq 0$. Similarly, we can obtain bounds for all components, leading to the inequality in the theorem.

Proof Sketch of Theorem 4.4: Theorem 4.3 bounds the gap of gain between the optimal paths for specific information gain and for its estimate. This bound is obtained by adding the gap of gain between optimal and approximated paths with estimated specific information gain.

REFERENCES

- [1] J. A. Placed, J. Strader, H. Carrillo, N. Atanasov, V. Indelman, L. Carlone, and J. A. Castellanos, "A survey on active simultaneous localization and mapping: State of the art and new frontiers," *IEEE Transactions on Robotics*, vol. 39, no. 3, pp. 1686–1705, 2023.
- [2] R. Zeng, Y. Wen, W. Zhao, and Y.-J. Liu, "View planning in robot active vision: A survey of systems, algorithms, and applications," *Comp. Visual Media*, vol. 6, p. 225–245, 2020.
- [3] A. Krause, A. Singh, and C. Guestrin, "Near-optimal sensor placements in gaussian processes: Theory, efficient algorithms and empirical studies," *J. Mach. Learn. Res.*, vol. 9, p. 235–284, jun 2008.
- [4] A. Krause and C. Guestrin, "Nonmyopic active learning of gaussian processes: an exploration-exploitation approach," in *Proceedings of the 24th International Conference on Machine Learning*, ser. ICML '07. New York, NY, USA: Association for Computing Machinery, 2007, p. 449–456. [Online]. Available: <https://doi.org/10.1145/1273496.1273553>
- [5] A. Singh, A. Krause, C. Guestrin, and W. J. Kaiser, "Efficient informative sensing using multiple robots," *Journal of Artificial Intelligence Research*, vol. 34, p. 707–755, Apr. 2009. [Online]. Available: <http://dx.doi.org/10.1613/jair.2674>
- [6] J. Binney and G. S. Sukhatme, "Branch and bound for informative path planning," in *2012 IEEE International Conference on Robotics and Automation*, 2012, pp. 2147–2154.
- [7] A. Viseras, D. Shutin, and L. Merino, "Robotic active information gathering for spatial field reconstruction with rapidly-exploring random trees and online learning of gaussian processes," *Sensors*, vol. 19, no. 5, 2019. [Online]. Available: <https://www.mdpi.com/1424-8220/19/5/1016>
- [8] C. Connolly, "The determination of next best views," in *Proceedings. 1985 IEEE International Conference on Robotics and Automation*, vol. 2, 1985, pp. 432–435.
- [9] A. Bircher, M. Kamel, K. Alexis, H. Oleynikova, and R. Siegwart, "Receding horizon "next-best-view" planner for 3d exploration," in *2016 IEEE International Conference on Robotics and Automation (ICRA)*, 2016, pp. 1462–1468.
- [10] L. Yoder and S. Scherer, *Autonomous Exploration for Infrastructure Modeling with a Micro Aerial Vehicle*. Cham: Springer International Publishing, 2016, pp. 427–440. [Online]. Available: https://doi.org/10.1007/978-3-319-27702-8_28
- [11] R. Border, J. D. Gammell, and P. Newman, "Surface edge explorer (see): Planning next best views directly from 3d observations," *2018 IEEE International Conference on Robotics and Automation (ICRA)*, pp. 1–8, 2018.
- [12] L. Schmid, M. Pantic, R. Khanna, L. Ott, R. Siegwart, and J. Nieto, "An efficient sampling-based method for online informative path planning in unknown environments," *IEEE Robotics and Automation Letters*, vol. 5, no. 2, pp. 1500–1507, 2020.
- [13] Z. Zhang, T. Henderson, V. Sze, and S. Karaman, "Fsmi: Fast computation of shannon mutual information for information-theoretic mapping," in *2019 International Conference on Robotics and Automation (ICRA)*, 2019, pp. 6912–6918.
- [14] B. Charrow, S. Liu, V. Kumar, and N. Michael, "Information-theoretic mapping using cauchy-schwarz quadratic mutual information," in *2015 IEEE International Conference on Robotics and Automation (ICRA)*, 2015, pp. 4791–4798.
- [15] T. Henderson, V. Sze, and S. Karaman, "An efficient and continuous approach to information-theoretic exploration," in *2020 IEEE International Conference on Robotics and Automation (ICRA)*, 2020, pp. 8566–8572.
- [16] R. Shrestha, F.-P. Tian, W. Feng, P. Tan, and R. Vaughan, "Learned map prediction for enhanced mobile robot exploration," in *2019 International Conference on Robotics and Automation (ICRA)*, 2019, pp. 1197–1204.
- [17] Y. Tao, E. Iceland, B. Li, E. Zwecher, U. Heinemann, A. Cohen, A. Avni, O. Gal, A. Barel, and V. Kumar, "Learning to explore indoor environments using autonomous micro aerial vehicles," in *2024 IEEE International Conference on Robotics and Automation (ICRA)*, 2024, pp. 15 758–15 764.
- [18] Y. Tao, Y. Wu, B. Li, F. Cladera, A. Zhou, D. Thakur, and V. Kumar, "Seer: Safe efficient exploration for aerial robots using learning to predict information gain," in *2023 IEEE International Conference on Robotics and Automation (ICRA)*, 2023, pp. 1235–1241.
- [19] G. Georgakis, B. Bucher, K. Schmeckpeper, S. Singh, and K. Daniilidis, "Learning to map for active semantic goal navigation," *arXiv preprint arXiv:2106.15648*, 2021.
- [20] H. Siming, C. D. Hsu, D. Ong, Y. S. Shao, and P. Chaudhari, "Active perception using neural radiance fields," in *2024 American Control Conference (ACC)*, 2024, pp. 4353–4358.
- [21] Y. Tao, X. Liu, I. Spasojevic, S. Agarwal, and V. Kumar, "3d active metric-semantic slam," *IEEE Robotics and Automation Letters*, vol. 9, no. 3, pp. 2989–2996, 2024.
- [22] A. Dosovitskiy and V. Koltun, "Learning to act by predicting the future," *arXiv preprint arXiv:1611.01779*, 2016.
- [23] X. Sun, Y. Wu, S. Bhattacharya, and V. Kumar, "Multi-agent exploration of an unknown sparse landmark complex via deep reinforcement learning," *arXiv preprint arXiv:2209.11794*, 2022.
- [24] D. S. Chaplot, D. Gandhi, S. Gupta, A. Gupta, and R. Salakhutdinov, "Learning to explore using active neural slam," *arXiv preprint arXiv:2004.05155*, 2020.
- [25] A. Slivkins, "Lecture notes: Bandits, experts and games (lecture 8)," 2016. [Online]. Available: <https://www.cs.umd.edu/~slivkins/CMSC858G-fall16/lecture8-both.pdf>
- [26] R. Li, H. Gao, M. Tancik, and A. Kanazawa, "Nerfacc: Efficient sampling accelerates nerfs," *arXiv preprint arXiv:2305.04966*, 2023.
- [27] M. Savva, A. Kadian, O. Maksymets, Y. Zhao, E. Wijmans, B. Jain, J. Straub, J. Liu, V. Koltun, J. Malik, et al., "Habitat: A platform for embodied ai research," in *Proceedings of the IEEE/CVF international conference on computer vision*, 2019, pp. 9339–9347.
- [28] A. Szot, A. Clegg, E. Undersander, E. Wijmans, Y. Zhao, J. Turner, N. Maestre, M. Mukadam, D. S. Chaplot, O. Maksymets, et al., "Habitat 2.0: Training home assistants to rearrange their habitat," *Advances in neural information processing systems*, vol. 34, pp. 251–266, 2021.
- [29] X. Puig, E. Undersander, A. Szot, M. D. Cote, T.-Y. Yang, R. Partsey, R. Desai, A. W. Clegg, M. Hlavac, S. Y. Min, et al., "Habitat 3.0: A co-habitat for humans, avatars and robots," *arXiv preprint arXiv:2310.13724*, 2023.
- [30] S. Folk, J. Paulos, and V. Kumar, "Rotorpy: A python-based multirotor simulator with aerodynamics for education and research," *arXiv preprint arXiv:2306.04485*, 2023.
- [31] B. Yamauchi, "A frontier-based approach for autonomous exploration," in *Proceedings 1997 IEEE International Symposium on Computational Intelligence in Robotics and Automation CIRA'97. Towards New Computational Principles for Robotics and Automation*. IEEE, 1997, pp. 146–151.
- [32] K. Chaney, F. Cladera, Z. Wang, A. Bisulco, M. A. Hsieh, C. Korpela, V. Kumar, C. J. Taylor, and K. Daniilidis, "M3ed: Multi-robot, multi-sensor, multi-environment event dataset," in *Proceedings of the IEEE/CVF Conference on Computer Vision and Pattern Recognition (CVPR) Workshops*, June 2023, pp. 4016–4023.
- [33] I. D. Miller, F. Cladera, T. Smith, C. J. Taylor, and V. Kumar, "Stronger together: Air-ground robotic collaboration using semantics," *IEEE Robotics and Automation Letters*, vol. 7, no. 4, 2022.
- [34] C. Bai, T. Xiao, Y. Chen, H. Wang, F. Zhang, and X. Gao, "Faster-lio: Lightweight tightly coupled lidar-inertial odometry using parallel sparse incremental voxels," *IEEE Robotics and Automation Letters*, vol. 7, no. 2, pp. 4861–4868, 2022.
- [35] E. Marder-Eppstein. (2024) ROS move_base package.
- [36] A. Roth, "Learning in games (and games in learning)," 2023. [Online]. Available: <https://www.cis.upenn.edu/~aaroht/GamesInLearning.pdf>